Anal. Bioanal. Electrochem., Vol. 15, No. 8, 2023, 650-667
https://www.doi.org/10.22034/abec.2023.707325

Analytical & Bioanalytical Electrochemistry

Full Paper

Investigating The Effect of Silane Compound Employment, as an Electrolyte Additive on The Electrochemical Performance and Improvement of Cathode Electrode Surface Properties with The Active Material $LiNi_{0.5}Co_{0.2}Mn_{0.3}O_2$ in Lithium Ion Battery

Seyed Mohammad Reza Milani Hosseini,* and Hadi Moradi

Department of Analytical Chemistry, Faculty of Chemistry, Iran University of Science and Technology, Tehran, Iran

*Corresponding Author, Tel.: +98(21)77491208
E-Mail: drmilani@iust.ac.ir

Received: 30 June 2023 / Received in revised form: 19 August 2023 / Accepted: 23 August 2023 / Published online: 31 August 2023

Abstract- Lithium-ion batteries have emerged as the preferred choice for rechargeable power sources due to their ability to deliver high voltage, high energy density, and minimal self-discharge, making them ideal for electronic devices and energy storage applications. Among the most commonly employed industrial lithium-ion batteries is the 18650 commercial battery, measuring 18x65 mm, renowned for its rechargeable capabilities. Nonetheless, their widespread use faces significant safety challenges when subjected to extreme thermal or electrical stress. This study aims to enhance the safety and electrochemical performance of 18650-type battery cells at room temperature while mitigating the flammability risks associated with their carbonate-based electrolytes by incorporating an eco-friendly additive, vinyl triethoxysilane (VTES). Introducing 5 vol.% VTES into the electrolyte proved to be the optimal composition, resulting in improved cycling performance. This improvement can be attributed to the formation of stable and uniform surface films on both cathode and anode surfaces. These findings underscore the promise of VTES as an additive to enhance the safety and electrochemical performance of lithium-ion batteries, even at an industrial scale. To quantitatively and qualitatively assess the impact and performance of the VTES organic silicon compound, a comprehensive set of thermal and electrochemical analyses, including EDX, SEM, LSV, CV, EIS, TGA/DSC, and SET, were conducted.

Keywords- Lithium-ion batteries; Rechargeable; Power source; vinyltriethoxysilane; Electrolyte Additive

1. INTRODUCTION

Lithium-ion batteries have garnered interest for their capacity to deliver elevated voltage, substantial energy density, and minimal self-discharge in electronic devices and energy storage applications [1,2]. Although liquid electrolyte setups have proven effective in commercial lithium-ion batteries, the heightened flammability of these liquid-based electrolytes can lead to thermal runaway issues in such batteries [3,4].

Furthermore, the performance of lithium-ion batteries is significantly impacted by the type of electrolyte employed, making it a pivotal factor. Consequently, enhancing the safety and electrochemical stability of electrolytes can have a positive influence on the overall safety and electrochemical performance of lithium-ion batteries. Numerous methods have been explored in pursuit of these objectives. Research in this area has concentrated on enhancing electrolyte safety and thermal stability through the use of safer solvents, electrolyte additives [5-9], organic phosphorus compounds [10-19], and nitrogen-containing organic compounds [20-24].

While these additives have the potential to enhance the safety of lithium-ion batteries, certain cases exhibit a decline in electrochemical performance. Moreover, some of these additives are prone to reduction on the electrodes, leading to a noticeable reduction in ionic conductivity, often attributed to their high viscosity. In the realm of research, there has been a particular emphasis on the utilization of film-forming agents, with a focus on organic phosphorus compounds [25-30] and a range of electrolyte additives [31-47]. These efforts aim to enhance the electrochemical stability of both the electrolyte and the electrodes within lithium-ion batteries.

Nonetheless, these additives come with certain drawbacks, such as causing environmental pollution or posing toxicity risks. Consequently, there is a need for innovative additives that are environmentally friendly in the context of lithium-ion batteries.

Organosilicon compounds hold significant importance due to their environmental compatibility. Researchers have explored these compounds as a means to enhance the safety and electrochemical stability of both the electrolyte and electrodes in lithium-ion batteries, achieved through the formation of a surface film on either the cathode or anode [48-56].

Regrettably, a few of these compounds present challenges due to their intricate synthesis processes. It's worth noting that the Si–O chemical bond exhibits greater strength and stability when compared to the C–O bond. As a result, organosilicon compounds assume a pivotal role as additives in lithium-ion battery electrolytes. One such example is vinyltriethoxysilane (VTES), which has been recognized as a safe additive and enhancer of electrolyte electrochemical performance, with documented use in half-cell lithium-ion batteries [57].

In this study, we explore the utilization of vinyl triethoxysilane (VTES) as an electrolyte additive (optimized at 5% by volume) to enhance the safety and electrochemical performance of 18650-type rechargeable Li-ion cells, measuring 18x65mm in size – a prevalent industrial battery. We conducted these investigations at room temperature. VTES exhibits remarkable

attributes such as high thermal stability, low viscosity, and minimal toxicity, rendering it capable of improving the thermal and electrochemical stability of the electrolyte in these cells. In this research, the incorporation of VTES composition into the production of lithium-ion batteries can serve as a near-ideal solution both technically and economically. Given that the cost of 100 ml of VTES composition is approximately $5, it becomes evident that the expense associated with each 18650 battery containing 5% VTES is remarkably low. Importantly, this marks the first instance of a silane compound being investigated as an electrolyte additive in an industrial 18650-type lithium-ion battery. The thermal analysis of self-extinguishing time rate (SET) and TGA/DSC indicates that the inclusion of VTES compound in the electrolyte decreases its susceptibility to self-combustion, ignition, and flammability. This enhances the thermal stability and safety of both the electrolyte and lithium-ion cells. Furthermore, electrochemical impedance tests demonstrate optimization in parameters, including Warburg impedance coefficient, charge transfer resistance, electrolyte ohmic resistance, alternating current density, and lithium-ion diffusion coefficient. Scheme 1 provides an illustration of the chemical structure of vinyltriethoxysilane (VTES).

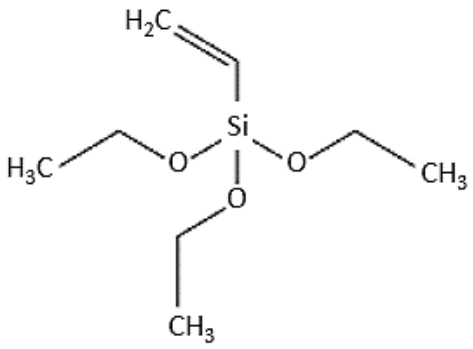

Scheme 1. Chemical structure of vinyltriethoxysilane (VTES)

2. EXPERIMENTAL SECTION

2.1. Materials

Vinyltriethoxysilane (VTES) was acquired from Merck Chemical Co. (Germany). The electrolyte solution was formulated by introducing varying quantities of VTES into a mixture of 1.0 M LiPF6 dissolved in ethylene carbonate (EC): ethyl methyl carbonate (EMC): dimethyl carbonate (DMC) in a 1:1:1 ratio, obtained from Guotai-Huarong New Chemical Materials Co., Ltd. (China). Diverse amounts of VTES were integrated into the empty electrolyte within an argon-filled glove box maintained at less than 1 ppm of H2O and O2. 18650-type battery cells with a capacity of 1,200 mAh were assembled,using 5 g of the aforementioned electrolyte with varying VTES content, graphite as the anode, and LiNi0.5Co0.2Mn0.3O2 as the cathode material. All 18650-type battery cells and CR2032 coin cells were constructed within an argon-filled glove box.

2.2. Measurements

The study assessed the flammability of electrolyte variants containing varying amounts of VTES by measuring their self-extinguishing times (SETs). Specifically, 0.83 grams of electrolyte with different VTES concentrations were ignited three times to calculate the average SETs, which were subsequently reported. To assess the heat release during the electrolyte decomposition, we employed differential scanning calorimetry (DSC) and thermogravimetric analysis (TGA) techniques, conducted under an argon (Ar) atmosphere with a heating rate of 10 °C/min, spanning from room temperature to 300 °C. The TGA/DSC thermal analyses were carried out using a Setaram Evolution TGA & DTA/DSC thermal analyzer from France. Additionally, linear sweep voltammetry (LSV) experiments were conducted using 1.0 M LiPF6/EC:EMC:DMC electrolytes with varying VTES content. A Pt wire (99.9%) served as the working electrode, while Li foil functioned as both the reference and counter electrodes. The voltage range explored was 0–6 V, and the scan rate utilized was 1 mV s^{-1}. Cyclic voltammetry (CV) was carried out by employing CR2032 coin cells with an Origa-Flex electrochemical workstation from France. The voltage range spanned from 2.6 to 4.5 V, and the scan rate was set at 0.1 mV s^{-1}. In addition, electrochemical impedance spectroscopy (EIS) was executed using the same workstation, involving 18650-type battery cells and covering a frequency range of 100 kHz to 10 mHz, utilizing a 5 mV amplitude. The impedance spectra were fitted using Z-view software. Lastly, charge and discharge performance assessments were performed on 18650-type battery cells using the Neware battery tester BTS-4000 system from China.

The 18650 battery cells underwent charging and discharging cycles within a voltage span of 3.0 to 4.2 V at current rates of 0.2 C, 0.5 C, and 1 C. We analyzed the cathode and anode surfaces using field-emission scanning electron microscopy (FE-SEM) with a TESCAN-VEGA3 instrument from the Czech Republic. Afterward, the electrodes were cleansed with anhydrous dimethyl carbonate (DMC) three times to eliminate any residual electrolyte components. Subsequently, they were subjected to vacuum drying at 40 °C for surface characterization.

3. RESULTS AND DISCUSSION

3.1. Thermal stability of electrolytes

To assess the efficacy of VTES in enhancing the safety of a lithium-ion battery electrolyte, we conducted SET, TGA, and DSC analyses. Figure 1 illustrates the SET values for a range of 1 M LiPF6 electrolytes, each with varying VTES concentrations. The SET for the electrolyte lacking VTES was 73.17 s g^{-1}, whereas the electrolyte containing 10 vol.% VTES exhibited a lower value of 56.77 s g^{-1}. As the VTES content increased, the electrolyte's SET progressively decreased. Generally, a reduced SET is indicative of decreased flammability [4]. Consequently,

the decreased SET in the VTES-modified electrolyte confirms its superior safety and reduced flammability compared to the VTES-free electrolyte.

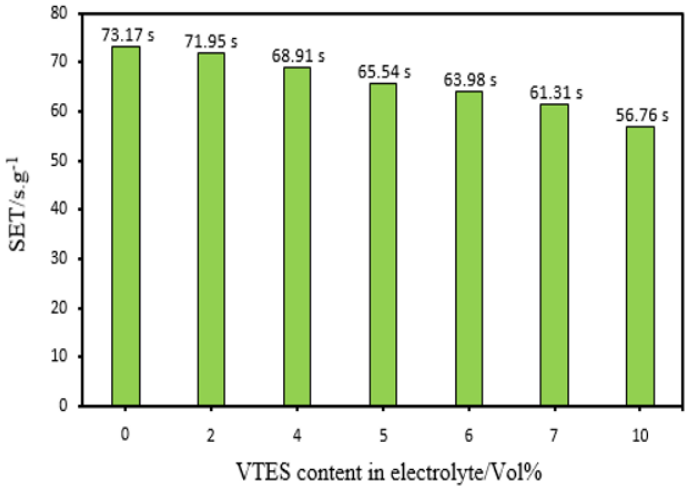

Figure 1. SETs of the 1 M $LiPF_6$ electrolytes without and with different VTES content

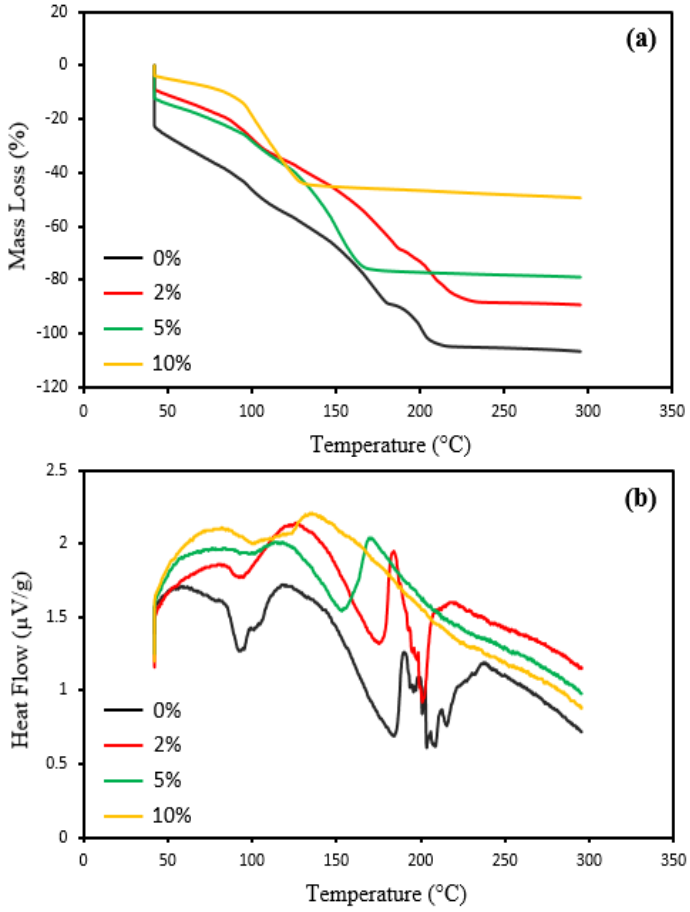

Figure 2. (a) TGA (b) DSC curves of the 1 M $LiPF_6$ electrolytes without and with different VTES content

Figures 2a and 2b display the TG and DSC curves, respectively, of 1 M LiPF6 electrolytes containing varying amounts of VTES. The TG curves reveal that within the 50–100 °C temperature range, the electrolyte with VTES exhibited a slower decomposition process compared to the one without VTES. Additionally, the DSC curves demonstrate a reduction in released heat as the VTES content increases. In terms of safety assessment, lower heat generation is a crucial parameter when analyzing DSC curves, as it signifies a safer electrolyte [58]. Therefore, VTES appears to enhance the thermal stability of the electrolyte, as suggested by these findings.

3.2. Electrochemical characterization of the electrolytes

Figures 3a and 3b display the linear sweep voltammograms of 1 M LiPF6 electrolytes, both with and without the addition of VTES. They also illustrate the electrochemical stability windows. Without VTES, the electrolyte begins to decompose at 4.7 V. However, when VTES is introduced at concentrations of 2%, 5%, 7%, and 10%, the decomposition thresholds shift to 5.0 V, 5.2 V, 4.6 V, and 4.4 V, respectively. Notably, the 5% VTES-containing electrolyte exhibits remarkable stability, showing no decomposition below 5.2 V. This suggests that VTES enhances the electrochemical stability of the electrolyte, providing a wider stability window for lithium-ion batteries.

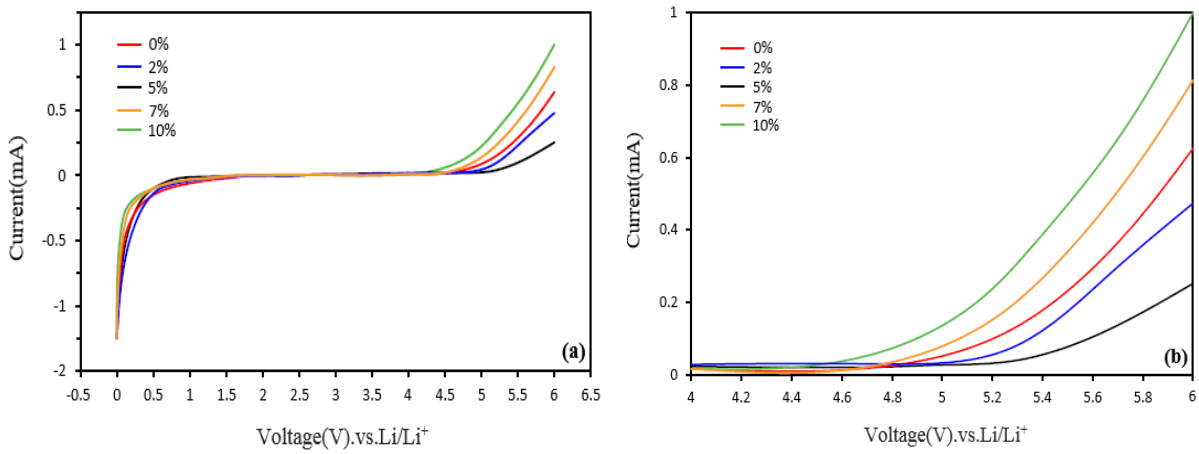

Figure 3. (a) Linear sweep voltammograms of 1 M $LiPF_6$ electrolytes without and with different VTES content; (b) Voltammograms of (a) with a larger magnification

3.3. Electrochemical performance

Figure 4 illustrates cyclic voltammetry (CV) curves for $LiNi_{0.5}Co_{0.2}Mn_{0.3}O_2$/Li coin cells employing 1 M $LiPF_6$ electrolytes, both with and without the inclusion of 5 vol.% VTES. In the initial cycle, CV curves of the VTES-containing electrolyte show a smaller difference in redox peak potentials (V=0.302 V) compared to the VTES-free electrolyte (V=0.387 V), indicating reduced polarization. Additionally, the diminished current peaks in the VTES-

containing electrolyte suggest that the surface film enhances stability but does not impact ionic conductivity.

Notably, the CV curves of the VTES-free electrolyte (as seen in Figure 4a) display a marked difference between the first and second cycles, likely due to the formation of a solid electrolyte interface (SEI) film during the initial cycle. In contrast, the first and second cycles of the electrolyte containing 5 vol.% VTES (Figure 4b) nearly overlap, possibly due to VTES replacing some electrolyte components, leading to the reversible formation of an SEI film [57].

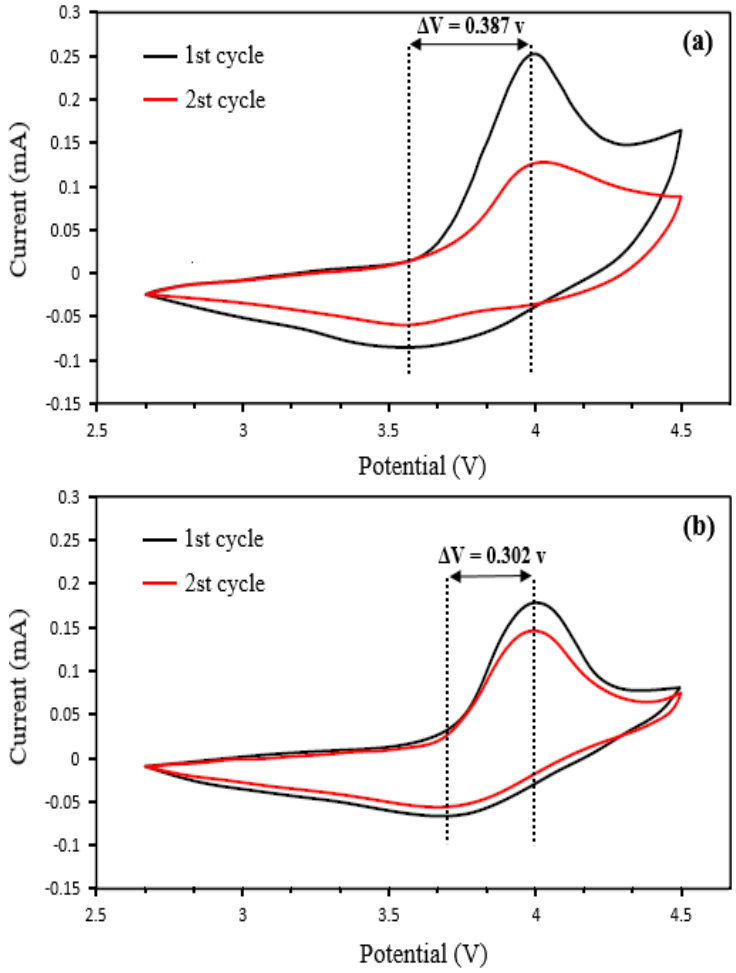

Figure 4. Cyclic voltammetry curves of the $LiNi_{0.5}Co_{0.2}Mn_{0.3}O_2$/Li coin cells with 1 M $LiPF_6$ electrolyte (a) without and (b) with 5 vol% VTES recorded at a scan rate of 0.1 mV s^{-1}

Figure 5a illustrates the performance of 18650-type battery cells with varying VTES content in 1 M LiPF6 electrolytes, tested at current rates of 0.2 C, 0.5 C, and 1 C over 100 cycles, with operation voltages set between 3.0 V and 4.2 V. Comparisons of the cycling performance of cells with different VTES content at these current rates are presented in Fig. 5b, 5c, and 5d, respectively.

Specifically, at a current rate of 0.2 C, the initial discharge capacities for cells containing 0%, 2%, 5%, 7%, and 10% VTES content are 2157.2 mAh, 2198.5 mAh, 2247.7 mAh, 2160.2

mAh, and 2098.9 mAh, respectively. The capacity retentions for these VTES content cells are 98.201%, 98.235%, 98.350%, 98.027%, and 97.188%, as shown in Figure 5b. At the current rate of 0.5 C, the initial discharge capacities for the VTES content cells mentioned are as follows: 2064.3, 2097.5, 2130.4, 2056.2, and 1935.9 mAh, with corresponding capacity retentions of 97.759%, 97.419%, 98.898%, 96.676%, and 92.120% as shown in Figure 5c. In Figure 5d, the initial discharge capacities for these VTES content cells are 1957.5, 1999.7, 2023.8, 1916.5, and 1641.7 mAh, with capacity retentions of 96.964%, 95.836%, 97.449%, 94.851%, and 91.885%, respectively.

According to the findings, the 18650-type battery cell with 5 vol.% VTES exhibits superior initial discharge capacity and capacity retention compared to cells containing varying VTES percentages across all current rates. Therefore, it can be concluded that 5 vol.% VTES is the optimal amount, providing favorable cycling performance for lithium-ion cells. These results align with the analysis presented in earlier sections.

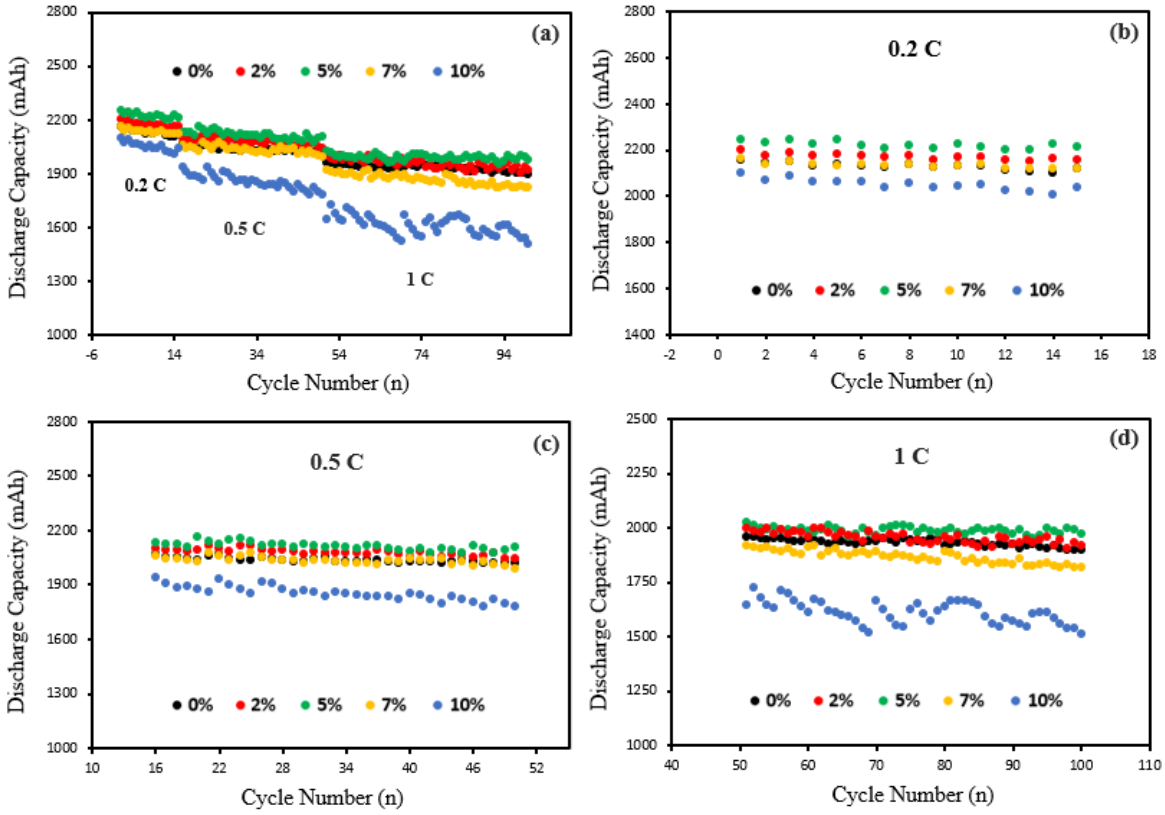

Figure 5. Cycling performance of the 18650-type battery cells with 1 M $LiPF_6$ electrolytes containing different VTES content (a) at current rates of 0.2 C, 0.5 C, and 1 C during 100 cycles. (b) at the current rates of 0.2 C (c) 0.5 C and, (d) 1C related to (a)

Figure 6a illustrates a comparison of discharge curves from the initial cycle of 18650-type battery cells. These cells utilize 1 M LiPF6 electrolytes with varying VTES content. A more detailed view of these curves can be seen in Figure 6b. The discharge capacities for cells

containing 0, 2, 5, 7, and 10 vol.% VTES content are 2157.2, 2198.5, 2195.9, 2247.7, 2166.9, 2160.2, and 2098.9 mAh in respective order, as evident from these figures.

Evidently, the cell with 5 vol.% VTES possesses a superior last discharge capacity compared to cells with different VTES contents. To confirm that 5 vol.% VTES is the optimal choice, the values of cells containing 4 and 6 vol.% VTES are also assessed, ensuring that 5 vol.% VTES yields the most suitable capacitive performance for 18650-type battery cells.

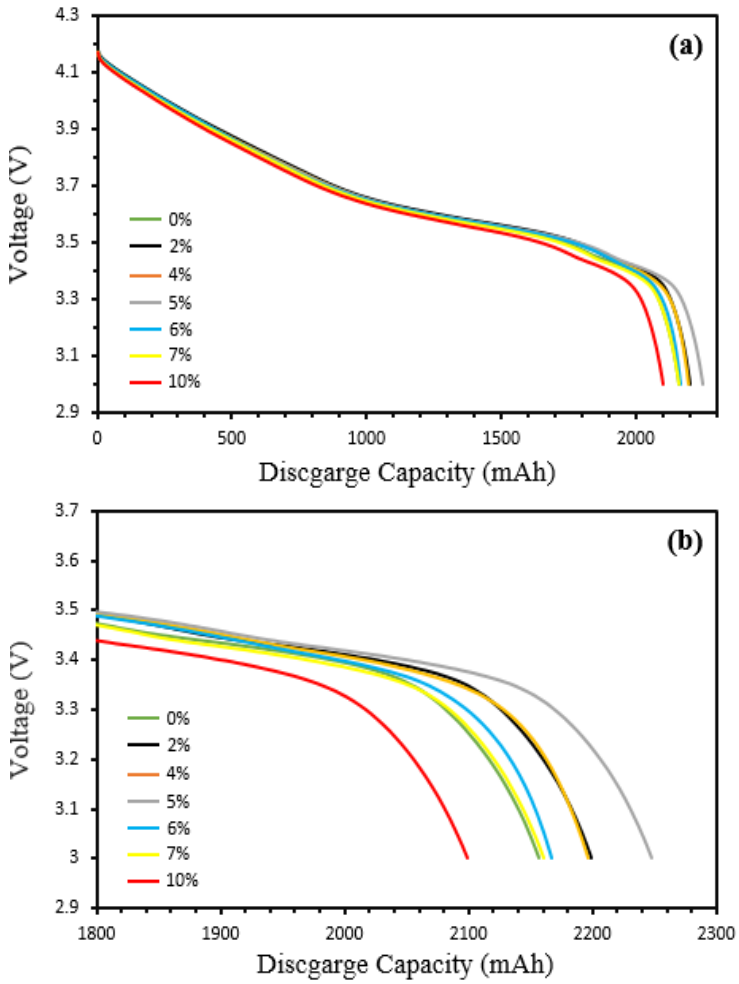

Figure 6. (a) Discharge curves related to the first cycle of the 18650-type battery cells with 1 M $LiPF_6$ electrolytes containing different VTES content (b) Curves of (a) with a larger magnification

Figures 7a and 7b depict impedance spectra acquired following a single cycle and 100 cycles, respectively, for 18650-type battery cells both with and without the addition of 5 vol.% VTES. The data includes experimental results represented by colored points and fitted data indicated by lines. Each spectrum displays two semi-circles and is fitted using the equivalent circuit illustrated in the inset of Figure 7a. The impedance parameters adhere to their conventional definitions [59-61]. The high-frequency semicircle typically corresponds to the

resistance associated with film resistance (R_{film}), while the medium-frequency semicircle represents charge-transfer resistance (R_{ct}). The low-frequency tail is attributed to Li+ migration resistance [62]. When fitting the EIS data (as shown in Figures 7a, 7b, and Table 1) for the cell containing 5 vol.% VTES after one cycle, the resulting values for R_{film} and R_{ct} were 0.0098 and 0.0151, respectively. These values are relatively higher compared to those obtained for the blank electrolyte cell, where R_{film} = 0.0074 and R_{ct} = 0.0084. This can be attributed to a thicker film formation in the VTES-added electrolyte cell, primarily due to electronic insulation. Consequently, this thicker film could lead to higher film and charge transfer impedances in the initial cycles of the cell. However, in the subsequent cycles (beyond the 100th charging), it's noteworthy that both R_{film} and R_{ct} values for the blank electrolyte cell (0.8271 and 8.8033, respectively) exceed those of the cell with 5 vol.% VTES (0.7762 and 8.4404, respectively). Notably, the substantial increase in R_{ct} is mitigated when 5 vol.% VTES is present. This suggests that the film, facilitated by VTES, acts as a more effective passivation layer to suppress additional electrolyte decomposition in later cycles. This phenomenon is depicted in Figure 7b, where the second semi-circle in the 5 vol.% VTES cell is smaller in comparison to the blank electrolyte cell. Furthermore, the Electrolyte resistance (Re) values after both one cycle and 100 cycles for the cells containing 5 vol.% VTES are lower than those for the blank electrolyte cells. This is attributed to the lower density and viscosity of VTES when compared to the electrolyte solvents. These findings strongly suggest that VTES has the potential to mitigate side reactions occurring on the electrode surfaces, which often impede the diffusion of Li^+ ions and lead to excessive growth of the electrode surface film. Consequently, this aids in maintaining a relatively stable structure of the electrode surface. As observed, these results align perfectly with the measurements discussed in the previous section.

Table 1. Fitting results of R_e, R_{film} and R_{ct} values obtained from the 18650-type cells with and without 5 vol.% VTES after 1 and 100 cycles.

Cycle number	VTES content in electrolyte/ Vol%	R_e (Ω cm^2)	R_{film} (Ω cm^2)	R_{ct} (Ω cm^2)
1^{st}	0%	0.1524	0.0074	0.0084
	5%	0.1448	0.0098	0.0151
100^{th}	0%	1.5050	0.8271	8.8033
	5%	1.3524	0.7762	8.4404

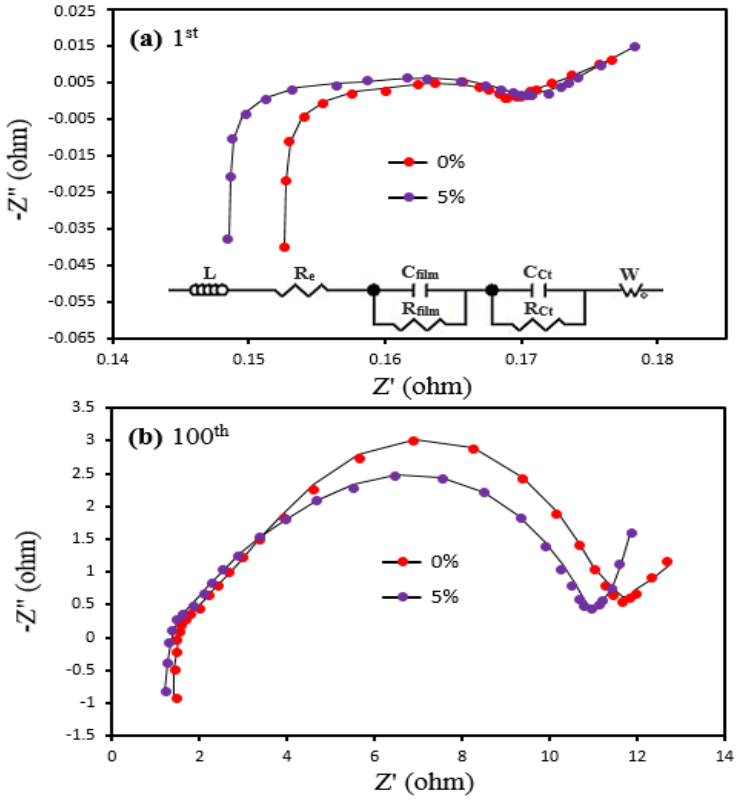

Figure 7. EIS spectra (Nyquist plot) obtained from the 18650-type battery cells with and without 5 vol.% VTES (a) after one cycle (b) after the 100 cycles. The equivalent circuit used for fitting EIS spectra of the full cells is shown in the inset

3.4. Surface characterization

To further illustrate the effectiveness of VTES, we conducted surface characterization of the cycled cathodes and anodes. In Figure 8, you can observe FE-SEM images depicting the surfaces of these cycled cathodes and anodes. As evident in Figures 8a and 8c, the surfaces of the cathode and anode that underwent cycling in the electrolyte without VTES exhibit a loose and heterogeneous appearance due to reactions with the electrolyte. In contrast, when employing the VTES-modified electrolyte (as shown in Figures 8b and 8d), a distinct layer is visible on the cathode and anode surfaces. We also conducted Energy dispersive X-ray (EDX) spectra and MAP (Material Analysis Program) imaging, which are presented in Figures 9, 10, and 11, respectively, related to these FE-SEM images. These images collectively demonstrate that the fundamental structure of the cathode and anode surfaces remains unchanged in the presence of VTES. Importantly, the original electrode structure remains stable within the 18650-type battery cells. Furthermore, these electrode surfaces have become notably more uniform and homogeneous.

As indicated by previously reported findings, the highest occupied molecular orbital (HOMO) energy level of VTES surpasses that of the EC, DMC, and EMC electrolyte solvent molecules. Consequently, VTES is more prone to oxidation compared to the solvents [58].

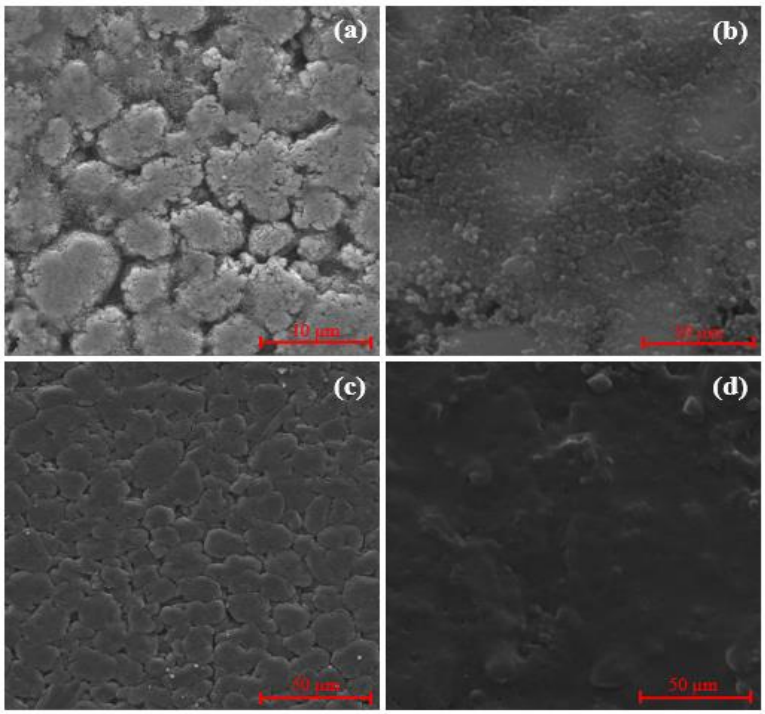

Figure 8. FE-SEM images of (a) $LiNi_{0.5}Co_{0.2}Mn_{0.3}O_2$ cathode surface without VTES and (b) with 5 vol.% VTES in 1 M $LiPF_6$. (c) Graphite anode surface without VTES and (d) with 5 vol.% VTES in 1 M $LiPF_6$ electrolytes after 20 cycles

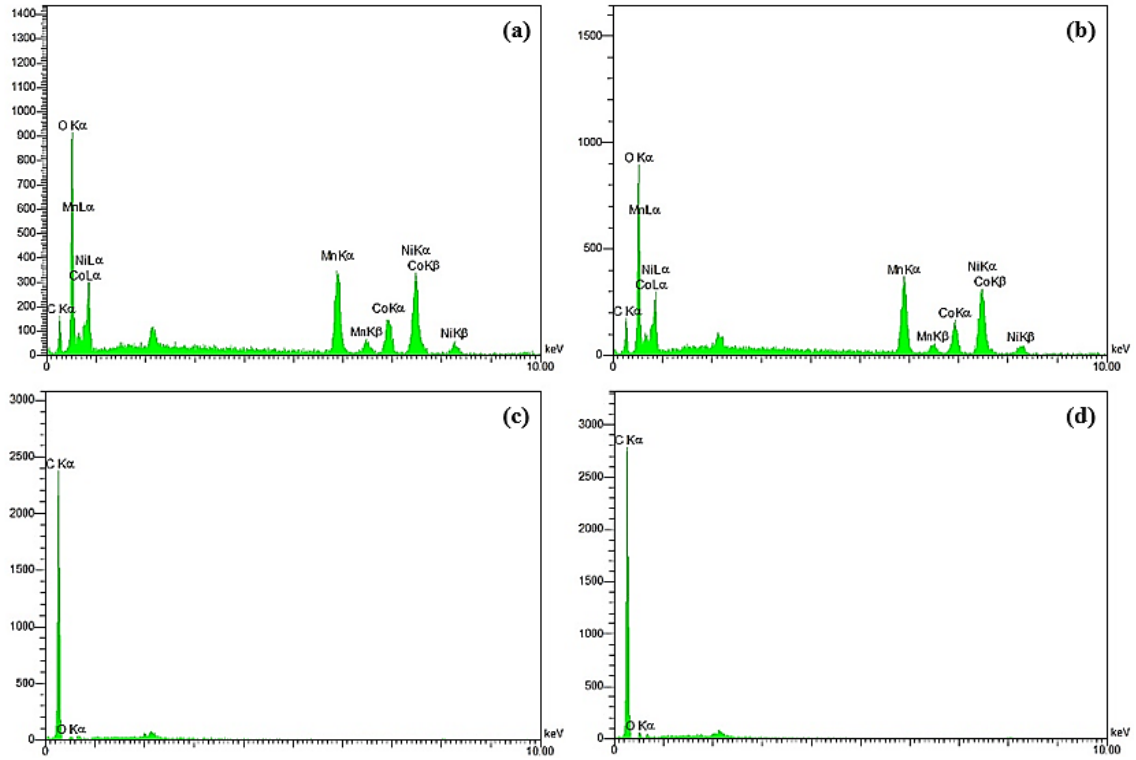

Figure 9. EDX analysis related to (a) $LiNi_{0.5}Co_{0.2}Mn_{0.3}O_2$ cathode surface without VTES and (b) with 5 vol.% VTES. (c) Graphite anode surface without VTES and (d) with 5 vol.% VTES in 1 M $LiPF_6$ electrolytes after 20 cycles

This observation suggests that VTES undergoes decomposition, thereby promoting the creation of a passivation film on the cathode surface. This aligns with previous research results [55]. Furthermore, VTES possesses a lower lowest unoccupied molecular orbital (LUMO) energy level in comparison to the EC, DMC, and EMC electrolyte solvent molecules. This implies that VTES is a more effective electron acceptor [58]. Consequently, VTES safeguards the anode by facilitating the formation of a uniform surface film, as depicted in Figure 8d.

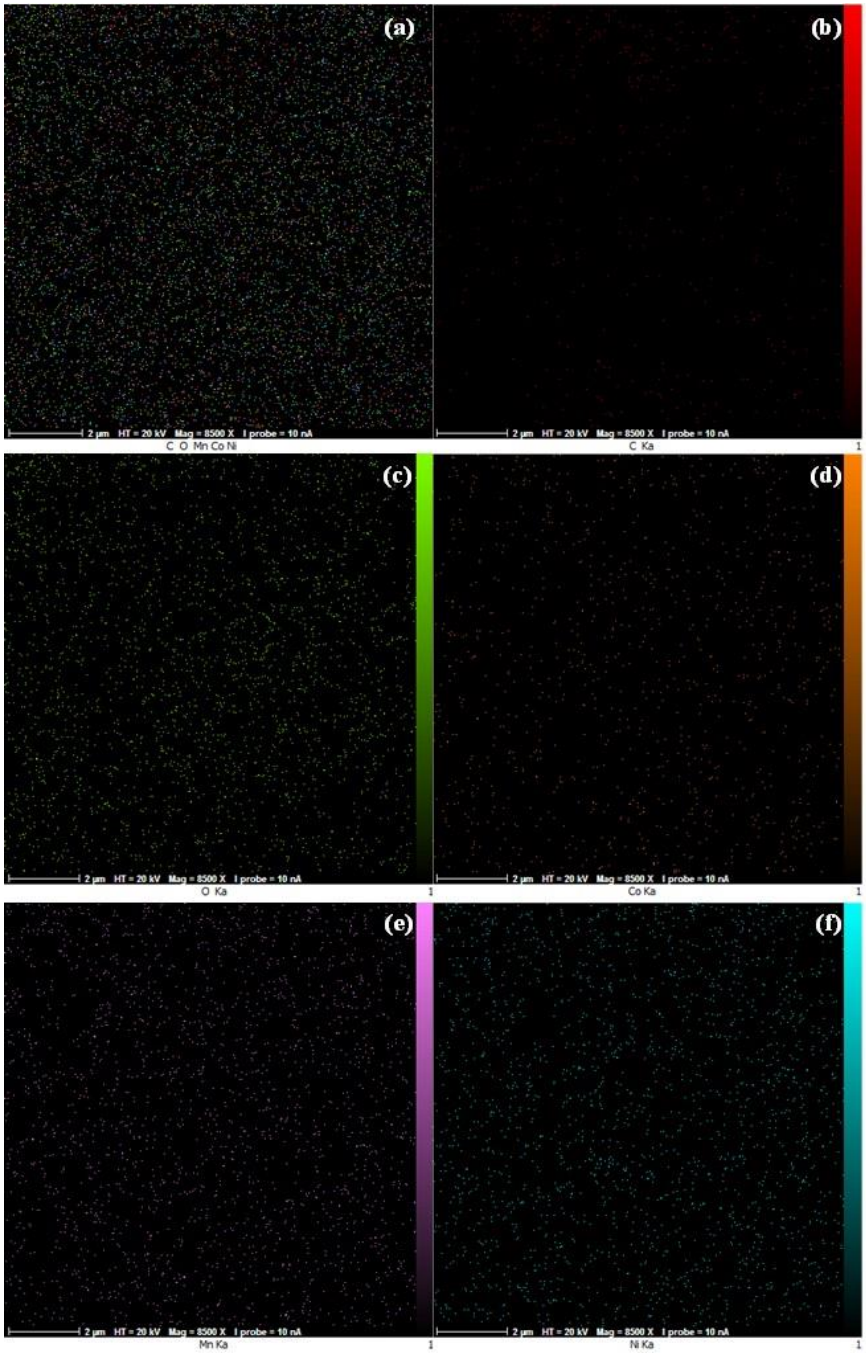

Figure 10. MAP analysis images of $LiNi_{0.5}Co_{0.2}Mn_{0.3}O_2$ cathode surface in 1 M $LiPF_6$ electrolyte without VTES related to (a) C, O, Mn, Co, and Ni, (b) C, (c) O, (d) Co, (e) Mn, and (d) Ni

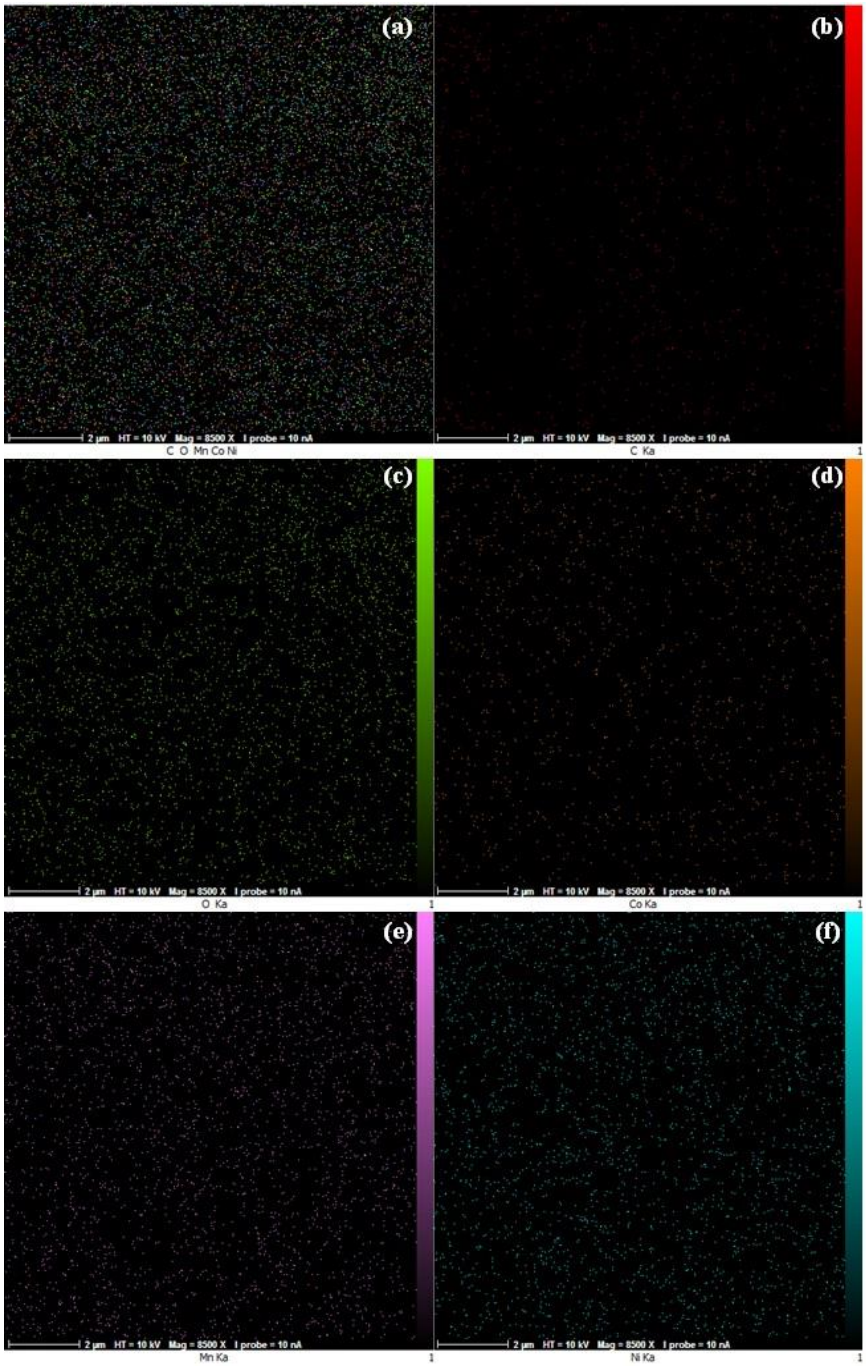

Figure 11. MAP analyze images of $LiNi_{0.5}Co_{0.2}Mn_{0.3}O_2$ cathode surface in 1 M $LiPF_6$ electrolyte with 5 vol.% VTES related to (a) C, O, Mn, Co, and Ni, (b) C, (c) O, (d) Co, (e) Mn, and (d) Ni

4. CONCLUSION

This study employed vinyltriethoxysilane (VTES) as an electrolyte additive, with an optimal content of 5 vol.%, to enhance the safety and electrochemical performance of 18650-type battery cells at room temperature. The electrolyte containing VTES demonstrates outstanding thermal stability, low viscosity, cost-effectiveness in preparation, and eco-

friendliness. Additionally, the modified electrolyte exhibits a broader electrochemical stability window compared to the unmodified one. The addition of VTES significantly reduces the self-discharge time (SET) of the electrolyte.

the cycling performance of cells containing 5 vol.% VTES is enhanced through the formation of stable and uniform surface films on both cathode and anode surfaces. These findings highlight VTES as a promising additive for improving the safety and electrochemical performance of lithium-ion batteries, even when implemented on an industrial scale.

Acknowledgments

We gratefully acknowledge financial support from the Research Council of Iran University of Science and Technology.

Declarations of interest

The authors declare no conflict of interest in this reported work.

REFERENCES

[1] Y. Nishi, J. Power Sources 100 (2001) 101.
[2] M.M. Thackeray, C. Wolverton, and E.D. Isaacs, Energy & Environ. Sci. 5 (2012) 7854.
[3] K. Xu, Chem. Rev. 104 (2004) 4303.
[4] J. Kalhoff, G.G. Eshetu, D. Bresser, and S. Passerini, ChemSusChem 8 (2015) 2154.
[5] R.P. Dunn, S.P.V. Nadimpalli, P. Guduru, and B.L. Lucht, J. Electrochem. Soc. 161 (2014) A176.
[6] X. Wang, C. Yamada, H. Naito, G. Segami, K. Kibe, J. Electrochem. Soc. 153 (2006) A135.
[7] J. Arai, J. Electrochem. Soc. 150 (2003) A219.
[8] E.G. Shim, T.H. Nam, J.G. Kim, H.S. Kim, and S.I. Moon, Electrochim. Acta 53 (2007) 650.
[9] Y. Kang, T. Yoon, S.S. Lee, J. Mun, M.S. Park, J.H. Park, S.G. Doo, I.Y. Song, and S.M. Oh, Electrochem. Commun. 27 (2013) 26.
[10] N. Yoshimoto, M. Egashira, and M. Morita, J. Power Sources195 (2010) 7426.
[11] K. Ciosek Högström, H. Lundgren, S. Wilken, T.G. Zavalis, M. Behm, K. Edström, P. Jacobsson, P. Johansson, and G. Lindbergh, J. Power Sources 256 (2014) 430.
[12] M.S. Ding, K. Xu, and T.R. Jow, J. Electrochem. Soc. 149 (2002) A1489.
[13] G. Xu, C. Pang, B. Chen, J. Ma, X. Wang, J. Chai, Q. Wang, W. An, X. Zhou, G. Cui, and L. Chen, Advanced Energy Mater. 8 (2018) 1701398.
[14] K. Xu, M. S. Ding, S. Zhang, J. L. Allen, and T. R. Jow, J. Electrochem. Soc. 150 (2003) A161.

[15] N. von Aspern, S. Röser, B. Rezaei Rad, P. Murmann, B. Streipert, X. Mönnighoff, S. D. Tillmann, M. Shevchuk, O. Stubbmann-Kazakova, G.V. Röschenthaler, S. Nowak, M. Winter, and I. Cekic-Laskovic, J. Fluorine Chem. 198 (2017) 24.
[16] X. Xia, P. Ping, and J.R. Dahn, J. Electrochem. Soc. 159 (2012) A1834.
[17] H. F. Xiang, H. Y. Xu, Z. Z. Wang, and C. H. Chen, J. Power Sources 173 (2007) 562.
[18] H. F. Xiang, H. W. Lin, B. Yin, C. P. Zhang, X. W. Ge, and C. H. Chen, J. Power Sources 195 (2010) 335.
[19] X. L. Yao, S. Xie, C. H. Chen, Q. S. Wang, J. H. Sun, Y. L. Li, and S. X. Lu, J. Power Sources 144 (2005) 170.
[20] C.E. Lee, V. Rajeev, and P. Jai, Electrochem. Solid-State Lett. 3 (2000) 63.
[21] T. Dagger, C. Lürenbaum, F.M. Schappacher, and M. Winter, J. Power Sources 342 (2017) 266.
[22] S. Bae, W. Shin, and D. Kim, Electrochim. Acta 125 (2014) 497.
[23] G. Xu, C. Pang, B. Chen, J. Ma, X. Wang, J. Chai, Q. Wang, W. An, X. Zhou, G. Cui, and L. Chen, Advanced Energy Mater. 8 (2018) 1701398 .
[24] X. Li, W. Li, L. Chen, Y. Lu, Y. Su, L. Bao, J. Wang, R. Chen, S. Chen, and F. Wu, J. Power Sources 378 (2018) 707.
[25] Y. Ren, M. Wang, J. Wang, and Y. Cui, Int. J. Electrochem. Sci. 13 (2018) 664.
[26] M. He, C.C. Su, C. Peebles, Z. Feng, J. G. Connell, C. Liao, Y. Wang, I. A. Shkrob, and Z. Zhang, ACS Applied Mater. & Interfaces 8 (2016) 11450 .
[27] M.S. Milien, U. Tottempudi, M. Son, M. Ue, and B.L. Lucht, J. The Electrochem. Soc. 163 (2016) A1369.
[28] Y.M. Song, J.G. Han, S. Park, K.T. Lee, and N.S. Choi, J. Mater. Chem. A 2 (2014) 9506.
[29] C. Wang, L. Yu, W. Fan, J. Liu, L. Ouyang, L. Yang, and M. Zhu, ACS Applied Energy Mater. 1 (2018) 2647.
[30] J. Xia, L. Madec, L. Ma, L.D. Ellis, W. Qiu, K.J. Nelson, Z. Lu, and J.R. Dahn, J. Power Sources 295 (2015) 203.
[31] J. Lan, Q. Zheng, H. Zhou, J. Li, L. Xing, K. Xu, W. Fan, L. Yu, and W. Li, ACS Applied Mater. Interfaces (2019).
[32] H. Bouayad, Z. Wang, N. Dupré, R. Dedryvère, D. Foix, S. Franger, J.F. Martin, L. Boutafa, S. Patoux, D. Gonbeau, and D. Guyomard, The Journal Phys. Chem. C 1189 (2014) 4634.
[33] P. Murmann, B. Streipert, R. Kloepsch, N. Ignatiev, P. Sartori, M. Winter, and I. Cekic-Laskovic, Phys. Chem. Chem. Phys. 17 (2015) 9352.
[34] B. Li, Y. Wang, W. Tu, Z. Wang, M. Xu, L. Xing, and W. Li, Electrochim. Acta 147 (2014) 636.

[35] C. Wang, L. Yu, W. Fan, J. Liu, L. Ouyang, L. Yang, and M. Zhu, ACS Applied Mater. Interfaces 9 (2017) 9630.
[36] X. Zheng, T. Huang, Y. Pan, W. Wang, G. Fang, and M. Wu, J. Power Sources 293 (2015) 196.
[37] H. Lee, T. Han, K. Y. Cho, M.-H. Ryou, and Y. M. Lee, ACS Applied Mater. Interfaces 8 (2016) 21366.
[38] W. Jia, C. Fan, L. Wang, Q. Wang, M. Zhao, A. Zhou, and J. Li, ACS Applied Mater. Interfaces 8 (2016) 15399.
[39] K.S. Kang, S. Choi, J. Song, S.G. Woo, Y. N. Jo, J. Choi, T. Yim, J.S. Yu, and Y.J. Kim, J. Power Sources 253 (2014) 48.
[40] S.J. Lee, J.G. Han, Y. Lee, M.H. Jeong, W.C. Shin, M. Ue, and N.S. Choi, Electrochim. Acta 137 (2014) 1.
[41] X. Zhao, Q.C. Zhuang, C. Wu, K. Wu, J.M. Xu, M.Y. Zhang, and X.L. Sun, J. Electrochem. Soc. 162 (2015) A2770.
[42] A. Nurpeissova, D.I. Park, S.S. Kim, and Y.K. Sun, J. Electrochem. Soc. 163 (2016) A171.
[43] Z. Wang, L. Xing, J. Li, M. Xu, and W. Li, J. Power Sources 307 (2016) 587.
[44] Z. Chen, C. Wang, L. Xing, X. Wang, W. Tu, Y. Zhu, and W. Li, Electrochim. Acta 249 (2017) 353.
[45] W. Tu, P. Xia, J. Li, L. Zeng, M. Xu, L. Xing, L. Zhang, L. Yu, W. Fan, and W. Li, Electrochim. Acta 208 (2016) 251.
[46] C. Peebles, M. He, Z. Feng, C.C. Su, L. Zeng, M. J. Bedzyk, P. Fenter, Y. Wang, Z. Zhang, and C. Liao, J. Electrochem. Soc. 164 (2017) A173.
[47] P. Dong, D. Wang, Y. Yao, X. Li, Y. Zhang, J. Ru, and T. Ren, J. Power Sources 344 (2017) 111.
[48] H.P. Zhang, Q. Xia, B. Wang, L.C. Yang, Y.P. Wu, D.L. Sun, C.L. Gan, H.J. Luo, A. W. Bebeda, and T. van Ree, Electrochem. Commun. 11 (2009) 526.
[49] L.L. Li, L. Li, B. Wang, L.L. Liu, Y. P. Wu, T. van Ree, and K.A. Thavhiwa, Electrochim. Acta 56 (2011) 4858.
[50] G. Schroeder, B. Gierczyk, D. Waszak, M. Kopczyk, and M. Walkowiak, Electrochem. Commun. 8 (2006) 523.
[51] C. Peebles, M. He, Z. Feng, C.C. Su, L. Zeng, M. J. Bedzyk, P. Fenter, Y. Wang, Z. Zhang, and C. Liao, J. Power Sources 180 (2008) 602.
[52] G. Schroeder, B. Gierczyk, D. Waszak, and M. Walkowiak, Electrochem. Commun. 8 (2006) 1583.
[53] T.J. Lee, J.B. Lee, T. Yoon, D. Kim, O.B. Chae, J. Jung, J. Soon, J.H. Ryu, J.J. Kim, and S. M. Oh, J. Electrochem. Soc. 163 (2016) A898.

[54] H. Xu, J. Shi, G. Hu, Y. He, Y. Xia, S. Yin, and Z. Liu, J. Power Sources 391 (2018) 113.
[55] J. Chen, H. Zhang, M. Wang, J. Liu, C. Li, and P. Zhang, J. Power Sources 303 (2016) 41.
[56] B. Deng, H. Wang, W. Ge, X. Li, X. Yan, T. Chen, M. Qu, and G. Peng, Electrochim. Acta 236 (2017) 61.
[57] R. Chen, Y. Zhao, Y. Li, Y. Ye, Y. Li, F. Wu, and S. Chen, J. Mater. Chem. A 5 (2017) 5142.
[58] G.G. Eshetu, S. Grugeon, G. Gachot, D. Mathiron, M. Armand, and S. Laruelle, Electrochim. Acta 102 (2013) 133.
[59] M.D. Levi, G. Salitra, B. Markovsky, H. Teller, D. Aurbach, U. Heider, and L. Heider, J. Electrochem. Soc. 146 (1999) 1279.
[60] D. Aurbach, M. D. Levi, and E. Levi, Solid State Ionics 179 (2008) 742.
[61] V. Muenzel, A. F. Hollenkamp, A. I. Bhatt, J. de Hoog, M. Brazil, D. A. Thomas, and I. Mareels, J. Electrochem. Soc. 162 (2015) A15920.
[62] Y. Lai, C. Ren, H. Lu, Z. Zhang, and J. Li, J. Electrochem. Soc. 159 (2012) A1267.